行政院國家科學委員會專題研究計畫　期中進度報告

低溫液相成長之氧化物奈米結構的電漿氣氛摻雜與光電性質研究(1/2)

計畫類別：個別型計畫
計畫編號：NSC94-2216-E-009-016-
執行期間：94 年 08 月 01 日至 95 年 07 月 31 日
執行單位：國立交通大學材料科學與工程學系(所)

計畫主持人：陳三元

報告類型：精簡報告
報告附件：出席國際會議研究心得報告及發表論文
處理方式：本計畫可公開查詢

中　華　民　國 95 年 5 月 28 日

低溫液相成長之氧化物奈米結構的電漿氣氛摻雜與光電性質研究(1/2):

陣列式氧化鋅奈米柱之電漿處理與光電性質研究

Plasma treatment and optical properties of ZnO nanorods arrays

計畫編號：NSC94-2216-E-009-016·

執行時間：94/08/01 ~ 95/07/31

主持人：陳三元 教授　　交通大學材料科學與工程學系

中文摘要

本研究利用化學溶液法在低溫環境中在鍍氧化鋅薄膜的矽基板上，經由過飽合析出成長高度陣列式排列的氧化鋅奈米柱，研究氧化鋅奈米柱在氫氣及氨氣電漿處理後其物理及化學特性的變化。化學特性分析中可以看出，氮與氫離子可以由氧化鋅奈米柱的缺陷路徑成功的擴散至奈米結構中，並且與鋅及氧元素產生化學鍵結反應。而在物理發光特性的研究上，氧化鋅奈米柱經過氫氣、氮氣及氨氣電漿處理後可降低其可見光放射強度並改善發光性質最高達 140 倍以上，但是在長時間的氨氣電漿處理後會因為微結構的崩解導致氧化鋅奈米線的光學性質變差。最後在氧化鋅奈米柱電性量測的研究方面，發現氧化鋅奈米柱經由適當的氨氣電漿處理後，可以成功的製備出具有小穿遂電壓(1.5 V)的 *P* 型氧化鋅奈米柱。經由本研究的結果顯示，可以利用常溫的水溶液合成法結合氣體電漿處理可以製備出規則排列的摻雜化氧化鋅奈米線，並且可應用在 *p-n* 接面和半導體異質結構的光電元件上。

關鍵字： 陣列化 ZnO 奈米柱、電漿處理、光電特性研究、異質結構

Abstract

Arrayed single crystal ZnO nanorods with different aspect ratios have been synthesized on silicon substrates buffered with ZnO film by low-temperature chemical solution method. The physical and chemical properties of zinc oxide nanorods after H_2 and NH_3 plasma treatments were systematically investigated. The obtained results implied that both nitrogen and hydrogen ion can diffuse into nanostructures to form chemical bonds with zinc and oxygen ions through the paths of defects. The ratio of the intensity of Ultraviolet (UV) emission (I_{UV}) to that of deep level emission (I_{DLE}) can be enhanced as 140 times as those of original ones. However, the optical properties would become poor because of the destruction of nanostructures after long time NH_3 plasma treatment. Finally, *p*-type ZnO nanorods with low tunneling voltage of 1.5 V can be successfully fabricated as proved by corresponding electrical measurement. Therefore, this study demonstrated that room temperature solution synthesis in combination with plasma treatment can be used to synthesize highly arrayed and oriented nitrogen-doped ZnO nanorods in the application of a *p-n* junction and semiconductor heterostructures for the optoelectronic devices.

Keywords: Allayed ZnO nanorods；plasma treatments; Optoelectronic properties ； Microstructure evolution；Heterostructures

1 Introduction

Although ZnO was reported to be the most potential material to realize the next generation

in UV semiconductor laser, most of the ZnO crystal is an *n*-type because it contains significant concentrations of shallow donors and native defects (Zn interstitials, O vacancies). Therefore, the control of defect states becomes an important issue for improvement of emission efficiency. However, unfortunately, most one-dimensional nanomaterials (nanowires or nanorods) have been paraded as "perfect-like" or "defects-free" nanocrystals so that there are rarely efficient methods to fabricate high-quality ZnO nano-scale nanostructures via doping the grown ZnO nanorods at lower temperatures because of no suitable diffusion paths except for in-situ growth of doped-ZnO via vapor-liquid-solid (VLS) process which usually takes place at high temperatures **[1,2]**. But, in our previous studies reveal that the single crystalline ZnO nanorods grown from aqueous solution contain many defects which can provide for the doping or incorporation of impurities into ZnO nanorods **[3]**. Therefore, in this work, a simple method by combining the aqueous solution process with hydrogen plasma treatment was proposed to develop high-quality well-aligned arrays of ZnO nanorods on organic substrates. The reaction between the plasma gas and ZnO nanorods will be also discussed.

2. Experimental

To grow the ZnO nanorods on silicon and organic polycarbonate (PC) substrates, ZnO buffered layer (thickness around 100 nm) was deposited on organic substrate by radio frequency (rf) magnetron sputtering using 99.99% ZnO as the target. After that, the ZnO-coated substrates were placed in a solution containing an equimolar (0.01M) aqueous solution of $Zn(NO_3)_2.6H_2O$ and hexamethylenetetramine (HMT) and reacted at 75^oC for 8-12 h. After grown, the ZnO nanorods were exposed to H_2 and NH_3 plasma for 30, 60, 120, 300, and 900 sec by inductively coupled plasma (ICP) system. For the plasma treatment, the substrate temperature, total gas pressure, ICP top power were maintained at 100^oC, 400 mTorr, 600 W, and 50 W, under H_2 plasma, and at 300^oC, 300 mTorr and 250 W under NH_3 plasma, respectively. Ohmic contacts were fabricated simply by sputtering indium (In) metal on *n*-ZnO films and ZnO nanorods. The area of contact electrodes and the average nanorod density were estimated to be about 1×10^{-4} cm^2 and 10^{10} cm^{-2}, respectively. The obtained ZnO nanorods were characterized with scanning electron microscopy, transmission electron microscopy. The chemical compositions were examined by X-ray photoelectron spectroscopy (XPS) after the samples were first sputtered for 90 sec to remove the surface containment by Ar ion. Photoluminescence of the ZnO nanorods were performed by the excitation from 325nm He-Cd laser at room temperature. I-V characteristics curve of the samples was measured by applying DC voltage to the device using a HP-4156 and each datum was averaged by measuring 10 times.

3. Results and discussion

3.1 High conductivity ZnO nanorods in hydrogen-plasma

Numerous prior investigations have reported that hydrogen ions not only could be more easily diffused into ZnO in the plasma-treated process and combine with other defects to form a shallow donor in ZnO, but also can increase the free electron concentration of ZnO to improve conductivity and strongly passivate the deep level emission to enhance the band edge luminescence. Therefore, **Figure 1** shows the SEM images taken from several samples with highly uniform and densely packed arrays of ZnO nanorods grown on flexible four-inch PC substrate (**Figure 1(a)**). The ZnO nanorods in **Figure 1(b)** present a well-defined hexagonal shape with a homogeneous diameter of approximately ~70 nm. The cross-sectional SEM image in **Figure 1(c)** demonstrates that the highly oriented ZnO nanorods with a uniform length of 500-520 nm are perpendicularly grown to the PC substrate. **Figure 1(d)** shows the high resolution TEM (HRTEM) image of the well-aligned ZnO nanorods grown on PC substrates with the corresponding selected area electron diffraction pattern shown in the inset. The fringe spacing between two adjacent lattice planes is about 0.52 nm which is nearly consistent with the *c*-axis parameter in hexagonal ZnO structure (c = 0.521 nm in ZnO wurtzite structure), indicating that <001> is the preferred growth direction for the ZnO nanorods. In addition, some stacking faults are also observed (marked with arrows) and these stacking faults seem not to affect the crystal quality of ZnO nanorods because the selected-area electron diffraction pattern in the inset of **Figure 1(d)** reveals that the ZnO nanorods still exhibit single crystalline structure.

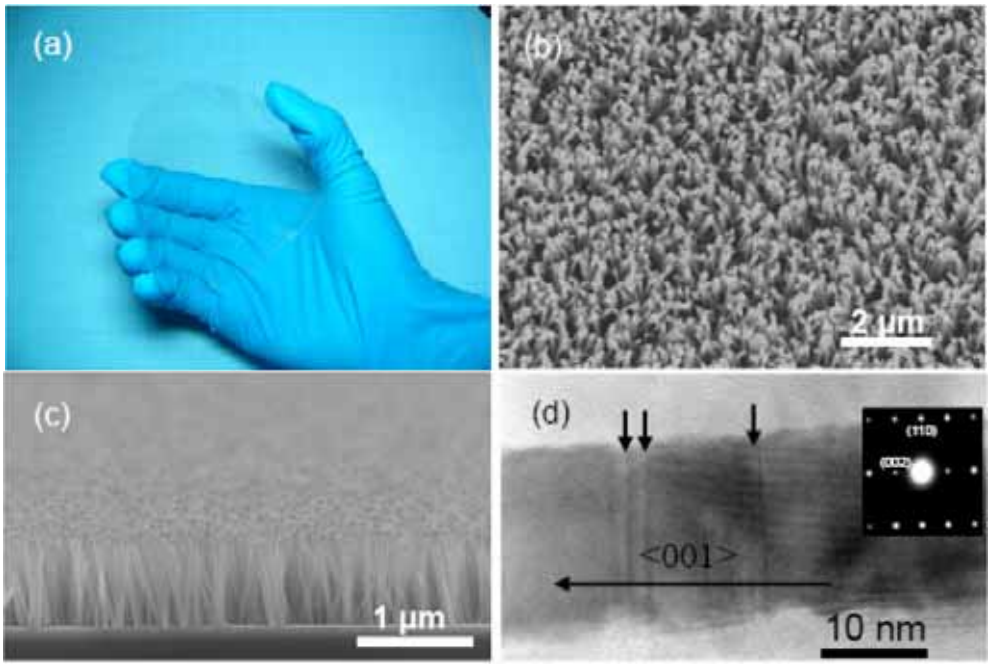

Figure 1: (a) Photograph of flexible PC grown with arrayed ZnO nanorods. (b) Low magnified top view image of ZnO nanorods. (c) Cross-sectional SEM image of ZnO nanorods grown on PC substrates. (d) High-resolution electron micrograph of ZnO nanorods with the SAED pattern shown in the inset.

Figure 2 illustrates the photoluminescence (PL) property of ZnO nanorods at room temperature. As shown in **Figure 2(a)**, the PL spectrum of non-plasma ZnO nanorods presents a weak ultraviolet (UV) emission peak at 3.28 eV and a relatively strong deep-level emission peak at 2.10 eV. Similar phenomena are also reported in the related literature **[4,5]**. The UV emission peak of ZnO is generally attributed to the exciton-related activity, and the deep level emission may be due to the transitions of native defects such as oxygen vacancies and zinc interstitials **[6,7]**. In addition, the imperfect boundaries and stacking faults of ZnO nanorods would cause the unstable surface status to trap impurities and further damage the optical property, especially as the diameter of ZnO nanorods was down to nano-scale. It was believed that those induced defects are probably related to the fast growth of the ZnO nanorods in the aqueous solution. In contrast, with the hydrogen plasma treatment, all the ZnO nanorods show much better PL property than that of non-plasma sample and the deep level emission was almost covered by the background signal in all plasma-treated samples. It was believed that the native defects or impurities contributing to visible transition can be passivated by H_2 plasma treatment, because the hydrogen atoms can be situated in various lattices positions and the most presumably stable position is the H configured at Zn-O bond center, which acts as a shallow donor.**[8]** Similar observations for the passivation of hydrogen plasma treatment on the visible emission of ZnO are also reported **[9]**. **Figure 2(b)** illustrates the ratio of peak intensity of Ultraviolet (UV) emission (I_{UV}) to that of deep level emission (I_{DLE}). The value of the relative PL ratio increases with the increase of plasma treatment duration up to 300 sec in all the samples and then becomes slightly decreased. A higher PL ratio implies that the plasma-treated ZnO nanorods exhibit higher optical quality. Moreover, it can be clearly observed that the crystal morphology of vertically well-aligned ZnO nanorods seems not to be affected by a lengthy plasma treatment even at 900 sec as revealed by the SEM images in the set of **Figure 2(b)**.

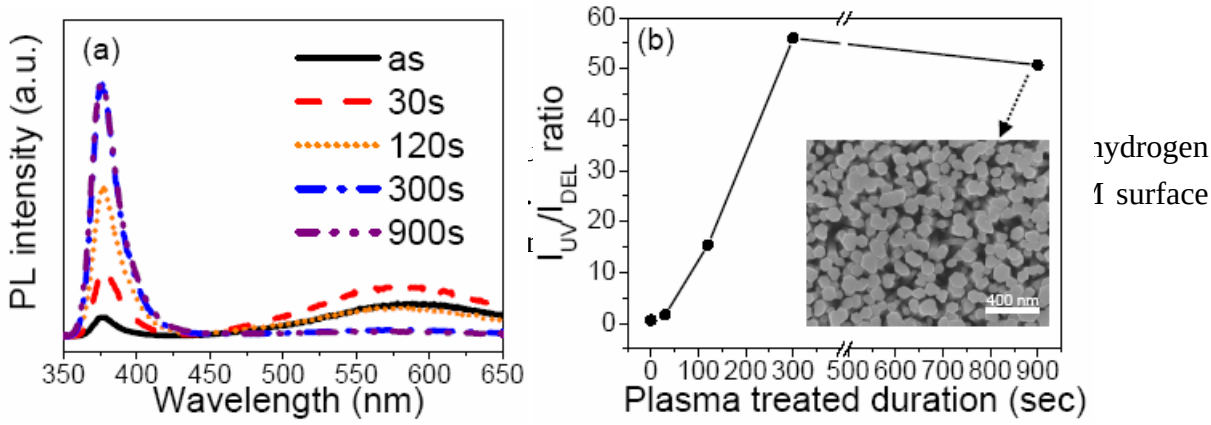

Figure 2: (a) PL spectra and (b) I_{UV}/I_{DEL} of ZnO nanorods with and without hydrogen plasma treatment at room temperature. The inset image of (b) shows the FESEM surface morphology of ZnO nanorods with hydrogen plasma treatment of t =900 sec.

Figure 3 shows the XPS core level spectra taken from the ZnO nanorods surface after the plasma treatment in H_2. As compared with the non-plasma sample, **Figure 3 (a)** illustrates that the peak shift of 0.2-0.3 eV toward higher binding energies was observed in Zn 2p spectrum for H_2 plasma-treated ZnO nanorods. This peak shift indicates the reduction of the surface band bending and this may be related to the doping or incorporation of H ions into ZnO nanorods **[10]**. Thus, the H_2 plasma treatment seems to partially recover or reduce surface defects, leading to the decrease of densities of surface states on ZnO nanorods. However, as the ZnO nanorods were treated with H_2-plasma duration more than 300 sec, the Zn 2p peak is shifted toward a higher binding energy around 0.5-0.8 eV. This phenomenon reveals that the surface band bending of ZnO nanorods was slightly changed by H_2 plasma treatment. Moreover, in comparison with non-plasma sample, the intensity of Zn 2p peak would decrease with the increase of the plasma duration. It might imply that local fine structure of ZnO nanorods could be changed and thus, more native defects were induced to raise the intensity of deep level emission. However, this phenomenon was not observed in our study. Therefore, it can be inferred that hydrogen plasma treatment might passivate these defect centers to suppress the deep level emission.

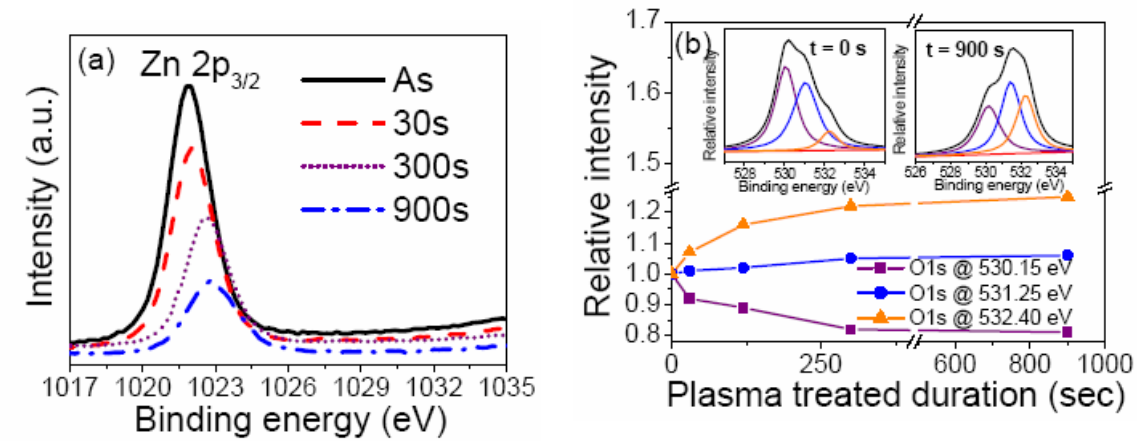

Figure 3: (a) Zn 2p spectra obtained from the ZnO nanorods with and without hydrogen plasma treatment. (b) Dependence of relative intensity ratio (O1s) of three fitted components centered at 530.15, 531.25, and 532.40 eV for the ZnO nanorods with and without hydrogen plasma treatment

In addition, the O1s peak presents different feature for the samples treated with various duration of hydrogen plasma as one can see in **Figure 3 (b)**. The typical O1s peak can be consistently fitted by three nearly Gaussian, centered at 530.15, 531.25, and 532.40 eV, respectively. Generally, the high binding energy component located at 532.40 is usually attributed to O-H bonds **[11]** which could be attributed to the absorbed hydrogen ions during the plasma treatment of ZnO nanorods. Furthermore, it can be observed that the peak intensity at high binding energy would increase as increasing plasma duration up to 300s and then it gets saturated. It indicates that hydrogen plasma treatment could efficiently

modify the surface states of ZnO nanorods by absorbing the hydrogen ions to reduce the unstable dangling bonds on the surface region of ZnO nanorods. **Figure 3(b)** also shows the variation of the medium binding energy component of O1s peak (centered at 531.25 eV) with plasma duration. The peak is generally associated with O^{2-} ions in oxygen deficient regions within the matrix of ZnO. It was observed that the peak intensity of this component does not obviously change with hydrogen plasma treatment. This indicates that the oxygen vacancies can not be reduced by H_2-plasma treatment to improve the optical properties in ZnO nanorods. To further understand the importance of hydrogen plasma treatment on the passivation effects of ZnO nanorods, the H_2-plasma samples were further annealed at various temperatures in nitrogen atmosphere. (Note: the post-annealed specimen were grown on Si substrate and then treated by hydrogen plasma at the same conditions as that grown on the flexible substrates.) It was found that the relative PL ratio would decrease drastically while the samples were annealed more than 400°C, as shown in **Figure 4**. Furthermore, the PL spectrum of the post-annealed ZnO nanorods was almost restored to that of original ZnO nanorods (ZnO nanorods without H_2 plasma treated). This implies that surface absorption and doping effects of hydrogen ions on ZnO nanorods can be recovered by thermal annealing process. Therefore, it can be concluded that both defect passivation and modification of surface state on hydrogen-plasma ZnO nanorods are responsible for the enhanced optical properties.

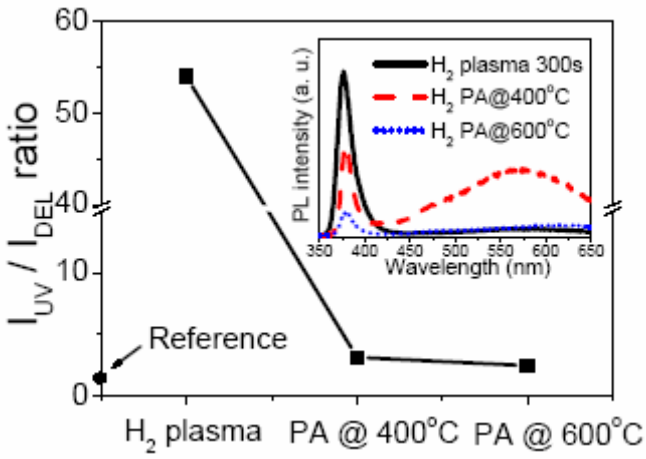

Figure 4: I_{UV}/I_{DEL} of ZnO nanorods (grown on ZnO film/ Si substrate) with hydrogen-plasma for 300 sec and then annealed at 400, and 600°C (PA@400 and PA@600 °C). The corresponding PL spectra of ZnO nanorods were shown in the inset.

Figure 5 shows the *I-V* curve for a homojunction of *n*-type ZnO nanorods (treated by H_2 plasma duration of 900 sec) on n-type ZnO films. The structure of In metal/ZnO nanorods/ZnO films/In metal/PC substrate was used for the I-V measurement of ZnO nanorods. It was found that the non-plasma ZnO nanorods present a higher resistivity about hundreds of MΩ, which is about 2 orders of magnitude larger than that reported in the literature for the naked single ZnO nanowire (above 3.5 MΩ). In contrast, when the ZnO

nanorods undergo hydrogen plasma treatment over than 300 sec, the resistivity of ZnO nanorods decrease by typically 5-6 orders of magnitude. It suggests that hydrogen plasma can efficiently raise the free electron concentration and increase the conductivity of ZnO nanorods. The above results reveal that with the H_2–plasma treatment on ZnO nanorods, both optical and electrical properties could be substantially improved and increased. This implies that incorporating hydrogen into ZnO nanorods not only passivates the native

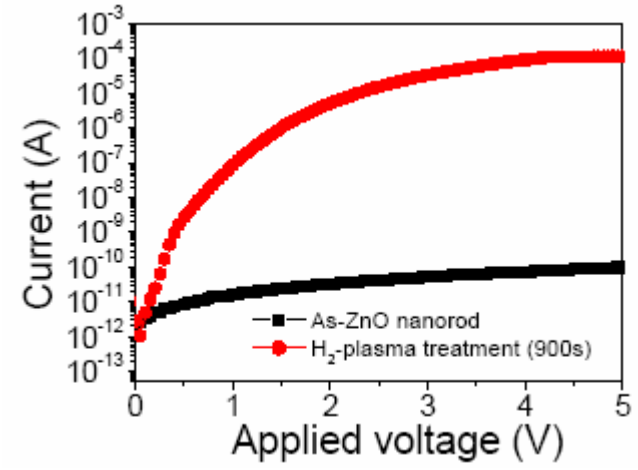

Figure 5: Comparison of *I-V* curves for the ZnO nanorods with and without H_2-plasma treated.defects but also acts as a shallow donor to improve the conductivity.

3.2 Rectifying behavior of ZnO nanorods by ammonia-plasma

The ZnO nanorods present single crystalline and a well-defined hexagonal plane with a homogeneous diameter of approximately 60-70 nm. The cross-sectional scanning electron microcopy (SEM) image in **Figure 6(a)** shows that the highly oriented ZnO nanorods with a uniform length of 500-520 nm are perpendicularly grown to the substrate. In addition, it was found that by controlling the experimental conditions, highly arrayed ZnO nanorods or nanowires with different aspect ratios can be grown from the chemical aqueous solution **[12]**. A close observation on the microstructure of the ZnO nanorods, as show in **Figure 6(b)**, reveals that the surface morphology of ZnO nanorods shows a waved shape structure with 0.5 ~ 1 nm roughnesses. In addition, some stacking faults are also observed (marked with arrows). However, these small surface roughness and stacking faults seem not to affect the crystal quality of ZnO nanorods because the selected-area electron diffraction pattern in the inset of **Figure 6(b)** reveals that the ZnO nanorods still exhibit a single crystalline structure. **Figure 6(b)** clearly describes the perpendicular directional growth of the ZnO nanorods where the singular fringes spacing is about 0.51nm, which is nearly consistent with the *c*-axis parameter in hexagonal ZnO structure (c = 0.521 nm in ZnO wurtzite structure), indicating that <001> is the preferred growth direction for the ZnO nanorods, in consistence with XRD patterns that show a single strong ZnO (002) peak at $2\theta = 34.4^{o}$.

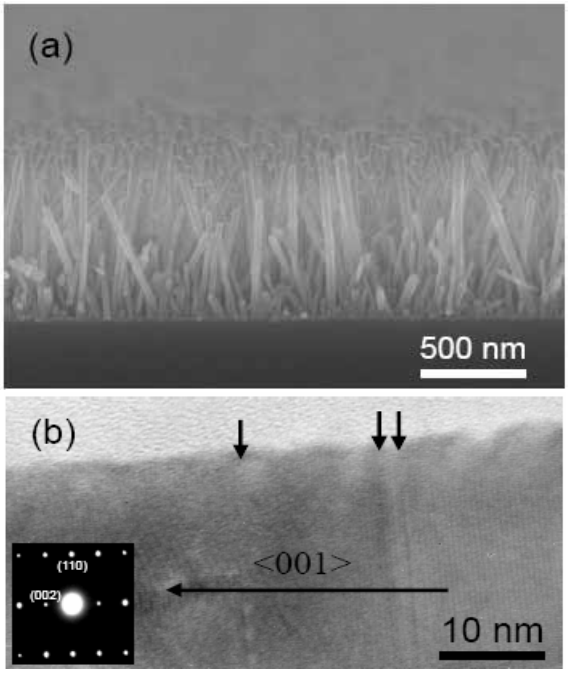

Figure 6: Cross-sectional scanning electron microcopy (SEM) micrograph of (a) ZnO nanorods/ZnO film/Si, (b) surface microstructure and stacking faults (marked with arrows) of ZnO nanorods. The inset image of (b) displays SAED pattern.

Figure 7(a) illustrates the photoluminescence (PL) property of ZnO nanorods at room temperature. The PL spectrum of non-plasma ZnO nanorods presents a weak ultraviolet (UV) emission peak at 3.28 eV and a relatively strong deep-level emission peak at 2.10 eV. The UV emission peak of ZnO is generally attributed to an exciton-related activity **[13]**, and the deep level emission may be due to the transitions of native defects such as oxygen vacancies and zinc interstitials. In addition, the imperfect boundaries in ZnO nanorods would cause the unstable surface status to trap impurities and further damage the optical property, especially for the nano-scale ZnO nanorods. In contrast, it was found that the peak intensity of the UV emission increases with the plasma duration up to 90 sec but the deep level emission in all plasma-treated samples tends to disappear, indicating that the native defects or impurities, contributing to visible transition, can be much reduced by NH_3 plasma treatment. As shown in **Figure 7(b)**, a maximum relative PL ratio (peak intensity of ultraviolet emission (I_{UV}) to that of deep level emission (I_{DLE})) shows up around 90-120 sec, implying that the plasma-treated ZnO nanorods exhibit much better PL properties than that of non-plasma sample. The improvement in the optical properties of ZnO nanorods with the plasma treatment may be attributed to the reduction of the defect concentration due to the occupation of N ions on the defect sites, i.e., oxygen vacancies, which will be further elucidated later. However, a further increase in plasma duration such as 180 sec would result in the decrease in the relative PL ratio that is probably related to the plasma etching as revealed by the SEM image in **Figure 7(c)** where the ZnO nanorods were deteriorated that

is in contrast to the ZnO nanorods with the plasma-treated duration less than 90 sec, well-aligned ZnO nanorods with well-defined hexagonal plane remains unchanged with an average length of 500 nm, similar to that without NH_3 plasma treatment.

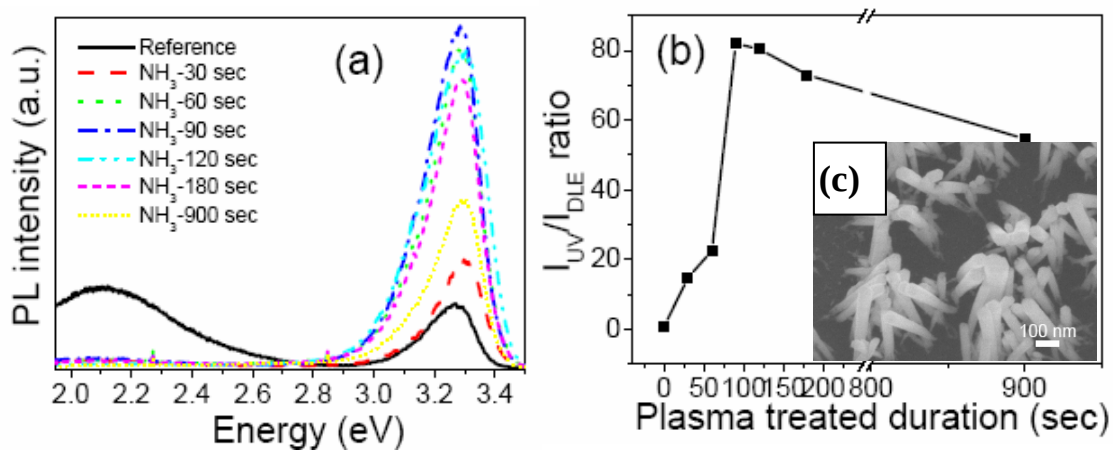

Figure 7. (a) Room-temperature PL spectra and (b) PL ratio of I_{UV}/I_{DEL} for ZnO nanorods with and without NH_3 plasma treatment. (c) FESEM surface morphology of ZnO nanorods with NH_3 plasma treatment of t =180 sec.

Figure 8 shows the relative intensity ratio of internal N (N_i) to surface N (N_f) dependent on etching time for the ZnO nanorods with NH_3 plasma treatment. No nitrogen signal was detected in the reference sample [see the inset of **Figure 8(a)**] but the N1s peak could be detected in plasma-treated ZnO nanorods from surface to internal region for the ZnO nanorods (duration at 90 sec). **(**Note: The N1s (~401 eV) internal signal was obtained by following the measurement steps. Firstly, ZnO nanorods were etched by Ar ion source and then the N1s signal of the etched ZnO nanorods can be detected. Next, both intensities of N1s signal (401 eV) for etched and non-etched nanorods were compared and considered as the internal and surface signals, respectively.) In addition, **Figure 8 (b)** illustrates the peak shift of 0.2-0.6 eV toward higher binding energies in Zn 2p spectrum for NH_3 plasma-treated ZnO nanorods as compared to that of the reference sample. This peak shift indicates the reduction of the surface band bending **[10]** and this may be related to the doping or incorporation of N ions into ZnO nanorods. The doped N atom could have the probability to occupy O sites to form the acceptor (N_O) in ZnO nanorods. Thus, the NH_3 plasma treatment seems to reduce the densities of the surface defects (**Figure 6(b)**) on ZnO nanorods. However, it was also observed in the inset of **Figure 8(b)** that as the ZnO nanorods were NH_3-plasma treated more than 180 sec, the Zn 2p peak is shifted toward a higher binding energy around 4-5 eV. This phenomenon implies that the surface band bending of the ZnO nanorods was strongly influenced by NH_3 plasma treatment and therefore, the structure morphology of ZnO nanorods would be probably changed as shown in **Figure 7(c)**.

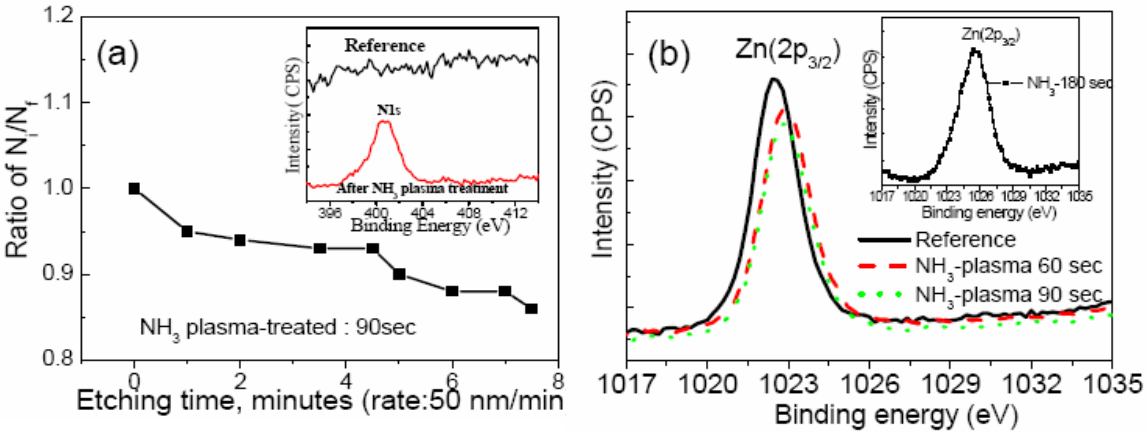

Figure 8: (a) Dependence of relative intensity ratio of internal N (N_i) to surface N (N_f) on etching time for the ZnO nanorods with the inset showing the N1s spectra obtained from the ZnO nanorods with and without NH_3 plasma treatment (t= 90 sec). (b) Zn 2p spectra obtained from the ZnO nanorods with and without NH_3 plasma treatment. The inset shows the Zn 2p3/2 spectra of ZnO nanorods with NH_3 plasma treatment of t=180 sec.

Based on the above discussion, a mechanism for the formation of p-type ZnO nanorods under NH_3-plasma treatment is tentatively proposed as follows. As can be seen in **Figure 6(b)**, imperfect boundaries (surface roughness) and many defects (stacking faults) were observed in the ZnO nanorods where N and H radicals (ions) can be easily doped into ZnO nanorods by thermal diffusion via the nature defect routes. In general, the H ions are more easily diffused into ZnO than N ions in the plasma-treated process and can combine with other defects to form a shallow donor in ZnO. However, according to the PL analysis, it was found that the luminescence properties were enhanced with the increase of plasma-treated duration up to 90 sec, indicating that the incorporation of H into ZnO nanorods does not show negative influence on the optical properties of ZnO nanorods in such short plasma duration. In other words, the improvement in optical property of ZnO nanorods can be primarily attributed to the reduction in surface defects and defect concentration of ZnO nanorods due to the occupation of N ions on the defect sites **[14]**. However, a long NH_3-Plasma treatment over 180 sec not only causes the plasma etching but also promotes the diffusion of H ions into the ZnO nanorods as well as increases the concentration of shallow donors to restrict the formation of p-type ZnO.

Figure 9 shows the I-V curve for a homojunction of *p*-type ZnO nanorods (treated by NH_3 plasma duration of 90 sec) on *n*-type ZnO films. The graph in the inset of **Figure 9** shows surface I-V characteristics using In and Au/In electrodes on both *n*- and *p*-type ZnO. For the linear dependences of I-V characteristics, the ohmic contacts are fairly confirmed. Rectification by *p*-*n* junction is clearly displayed. The threshold voltage appears at 1.5 V under forward bias and it is almost half of the band gap energy of ZnO. It was also found

that the I-V curve presents a little leakage current in reverse bias and this could be due to incomplete contact between some nanorods and contact metal electrode. Further experiments are required to understand the possible origin of the rectifying behavior with such a smaller threshold voltage. Nevertheless, the I-V characteristics of nitrogen-doped ZnO nanorods supports that the current approach is a valuable one to fabricate ZnO nanorods for *p*-*n* junction device application.

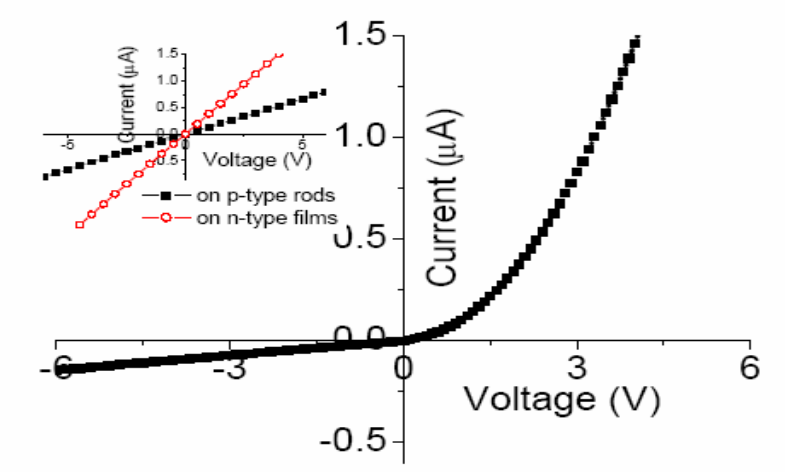

Figure 9: I-V curves for a *p*-*n* homojunction formed by *p*-type ZnO nanorods grown on *n*-type ZnO films. Inset show the Ohmic contacts on *n*-type and *p*-type ZnO.

4 Summary

We have developed well-aligned arrays ZnO nanorods on four-inch PC organic substrates buffered with ZnO film by combining a simple chemical solution at low temperatures with H_2 plasma treatment. The photoluminescence spectra indicate that the optical quality of the ZnO nanorods can be much improved by H_2 plasma treatment as evidenced by the remarkable increase in the ultraviolet emission intensity. The I-V results suggest that *n*-type ZnO nanorods with a higher conductivity can be obtained by combining the chemical solution process with hydrogen plasma treatment.

The XPS analysis shows that the nitrogen ions can be doped into ZnO nanorods through surface adsorption or defect routes under NH_3 plasma treatment. The native defects of the ZnO nanorods can be effectively reduced and the optical property can be much improved. Moreover, the electrical transport data reveal that *p*-type ZnO nanorods with a smaller threshold voltage of 1.5 V can be obtained by combining the chemical solution process with NH_3 plasma treatment.

Acknowledgment:

The authors gratefully acknowledge the National Science Council of Taiwan for its financial support through Contract No. NSC-94-2216-E-009-016.

References:

[1] Y. Q. Chang, D. B. Wang, X. H. Luo, X. Y. Xu, X. H. Chen, L. Li, C. P. Chen, R. M. Wang, J. Xu, D. P. Yu, *Appl. Phys. Lett.* **83** (2003) 4020.

[2] J. J. Wu, S. C. Liu, M. H. Yang, *Appl. Phys. Lett.* **85** (2004) 1027.

[3] C. C. Lin, H. P. Chen, and S. Y. Chen, *Chem. Phys. Lett.* **404** (2005) 30.

[4] M. H. Huang, Y. Wu, H. Feick, N. Tran, E. Weber, P. Yang, *Adv. Mater.* **13** (2001) 113.

[5] W.T. Chiou, W.Y. Wu, J.M. Ting, *Diam. Relat. Mater.* **12(10-11)** (2003) 1841.

[6] A. F. Kohan, G. Ceder, D. Morgan, and C. G. Van de Walle, *Phys. Rev. B* **61** (2000) 15019.

[7] C. G. Van de Walle, *Physica B* **308–310** (2001) 899.

[8] D. H. Lee and J. D. Joannopoulos, *Phys. Rev. B* **24** (1981) 6899.

[9] N. Ohashi, T. Ishigaki, N. Okada, T. Sekiguchi, I. Sakaguchi, and H. Haneda, *Appl. Phys. Lett.* **80** (2002) 2869.

[10] K. Ozawa and K. Edamoto, *Surf. Sci.* **524** (2003) 78.

[11] J. C. C. Fan, and J. B. Goodenough, *J. Appl. Phys.* **48** (1977) 3524.

[12] S. C. Liou, C. S. Hsiao, S. Y. Chen, *J. Crystal Growth* **274** (2004) 438.

[13] D. M. Bagnall, Y. R. Chen, Z. Zhu, T. Yao, S. Koyama, M. Y. Shen, T. Goto, *Appl. Phys. Lett.* **70** (1997) 2230.

[14] D. Li, Y. H. Leung, A. B. Djurisic, Z. T. Liu, M. H. Xie, S. L. Shi, S. J. Xu, W. K. Chen, *Appl. Phys. Lett.* **85** (2004) 1601.